

# Morphology and Magnetic Properties of Fe<sub>3</sub>O<sub>4</sub> and Au@Fe<sub>3</sub>O<sub>4</sub> Nanoparticles Synthesized by Pulsed Plasma in Liquid

Zhazgul Kelgenbaeva, Emil Omurzak, Saadat Sulaimankulova, and Tsutomu Mashimo

**Abstract**—Spherical shaped magnetite (Fe<sub>3</sub>O<sub>4</sub>) and Au@Fe<sub>3</sub>O<sub>4</sub> nanoparticles were successfully synthesized from Fe electrodes immersed in water with CTAB surfactant and HAuCl<sub>4</sub> solution using simple method-pulsed plasma in liquid, without the use of dopants or special conditions for stabilization. Vibrating sample magnetometer indicated ferromagnetic behavior of particles at room temperature with coercivity and saturation magnetization of (H<sub>c</sub>=105 Oe, M<sub>s</sub>=6.83 emu/g) for Fe<sub>3</sub>O<sub>4</sub> and (H<sub>c</sub>=175, M<sub>s</sub>=3.56emu/g) for Au@Fe<sub>3</sub>O<sub>4</sub> nanoparticles. Structure and morphology of nanoparticles were characterized by X-ray Diffraction analysis and HR-TEM measurements. The cytotoxicity of nanoparticles was indicated using a XTT assay to be very low (cell viability: 98-89% with Fe<sub>3</sub>O<sub>4</sub> and 99-91% for Au@Fe<sub>3</sub>O<sub>4</sub> NPs).

**Keywords**—Magnetite, Gold coated magnetite, Nanoparticles, Pulsed Plasma in Liquid, Cytotoxicity.

## I. INTRODUCTION

RESENT studies suggest that magnetic nanoparticles can bind to bacteria [1], protein [2], and enzyme [3] and could be directed to an organ, tissue, or cancer tumor by using an external magnetic field [4]. There are several types of iron oxide nanoparticles, namely maghemite, magnetite and haematite, among which magnetite is very promising because of its proven biocompatibility [5]. Encapsulation at nanometric level of iron oxide particles with noble metals, like gold or silver, allow for biocompatibility because of the good tolerance of the human body to these noble metals [6]. Also, iron oxide alone in physiological media is unstable, resulting in oxidation, aggregation and precipitation. A coating layer is needed to improve their biocompatibility, functionality and stability [7]. By using both iron oxide and gold as a single drug delivery vehicle, a multifaceted system can be developed which exploits the surface chemistry of the gold whilst retaining the magnetic character of the iron oxide, allowing for biologically sound drug delivery and imaging.

Here we report the synthesis of magnetite (Fe<sub>3</sub>O<sub>4</sub>) and Au@Fe<sub>3</sub>O<sub>4</sub> nanoparticles using pulsed plasma in liquid method

Zh. Kelgenbaeva is with the Graduate School of Science and Technology of Kumamoto University, Kumamoto, Japan (phone: +818046945860; fax: +81 96 342 3293; e-mail: jaza-86@mail.ru).

E. Omurzak is with the Priority Organization for Innovation and Excellence, Kumamoto University, Japan. (e-mail: emil@kumamoto-u.ac.jp)

S. Sulaimankulova is with the Institute of Chemistry and Chemical Technology, National Academy of Science of Kyrgyzstan (e-mail: satoba@mail.ru)

T. Mashimo is with the Shock Wave and Condensed Matter Research Center, Kumamoto University (e-mail: mashimo@gpo.kumamoto-u.ac.jp)

and their physicochemical properties. Pulsed plasma in liquid (PPL) combines physical (spark discharge) and chemical (surrounding liquid) processes, which provide us a number of advantages (simple, one-step, low-energy and versatile) for the synthesis of various kinds of nanomaterials [8]. The main challenge in this method is obtaining well-defined chemical compositions in the bulk and at the surface of the nanoparticles.

## II. EXPERIMENTAL

### A. Sample Preparation

The PPL experimental set-up (Fig.1) consists of two parts: a low voltage alternating current (AC) electric power supply and a glove box comprising electrodes submerged in liquid. For the experiments, rod shaped Fe electrodes with purity of 99.9% (Rare Metallic Co., Ltd) were immersed in a 200ml Pyrex beaker filled with a liquid. The liquid was water mixed with 1.0mM of 1n-Hexdecylpyridinium Bromide monohydrate «CTAB» (C<sub>21</sub>H<sub>40</sub>BrNO) (Cica-Reagent) for the Fe<sub>3</sub>O<sub>4</sub> samples preparation; and water with HAuCl<sub>4</sub> (Cica-Reagent) for the preparation of Au@Fe<sub>3</sub>O<sub>4</sub> samples. The gap between electrodes was about 1mm; duration of a single discharge was about 10μs and peak current about 100A. The AC electric power (200V, 6A) was applied for 1h in each experiment, and then reactor was cooled to room temperature. Samples were separated from the liquid with aid of centrifuge IEC61010-2-020, KUBOTA with 40×10<sup>2</sup>rpm speed for 20min, and then dried. The resulting Fe<sub>3</sub>O<sub>4</sub> powder was dark in color; the Au@Fe<sub>3</sub>O<sub>4</sub> nanopowder was also dark but sparkled due to the presence of gold.

### B. Sample Characterization

Obtained samples were characterized by classical techniques: X-ray diffraction (XRD: Rigaku RINT-2500HV, Cu-Kα, λ=1.5406Å) operated at 40kV and 200mA for structural analysis, vibrating sample magnetometer (VSM: Riken Denshi Co., Ltd) for studying magnetic properties. Morphology and dispersity of nanomaterials were analyzed using high resolution transmission electron microscopy (HR-TEM: Philips Tecnai F20 S-Twin, at 200keV). Cytotoxicity of Fe<sub>3</sub>O<sub>4</sub> and Au@Fe<sub>3</sub>O<sub>4</sub> nanoparticles was evaluated using a mammalian endothelial cell line, HeLa cells.

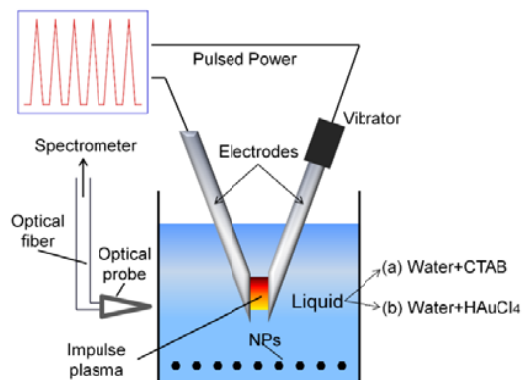


Fig. 1 Experimental set-up of pulsed plasma in liquid (PPL)

### III. RESULTS AND DISCUSSION

Phase composition and crystal structure of samples were examined by XRD, and effective tool to determine the phase, crystallinity and purity of samples prepared under various conditions. Fig. 2 shows XRD pattern of (a)  $\text{Fe}_3\text{O}_4$  sample and (b)  $\text{Au}@/\text{Fe}_3\text{O}_4$  samples synthesized by pulsed plasma in liquid. In Fig. 2a intensive characteristic reflections can be indexed as the face centered cubic structured  $\text{Fe}_3\text{O}_4$  with Fd-3m space group which is in accordance with the JCPDS card no 19-0629. No obvious impurity can be detected in pattern indicating the pure phase of samples. The diffraction peaks (Fig. 2b) at  $38.2^\circ$ ,  $44.4^\circ$ ,  $64.5^\circ$ , and  $77.6^\circ$  are attributed to gold, which can be indexed to 111, 200, 220 and 311 lattice planes of gold in a cubic phase (JCPDS card no 65-2870) and reflections at  $35.42^\circ$ ,  $43.05^\circ$ ,  $53.49^\circ$ ,  $57.03^\circ$ ,  $62.74^\circ$  and  $74.24^\circ$  corresponded to magnetite, indicating the presence of both  $\text{Fe}_3\text{O}_4$  and gold in the sample.

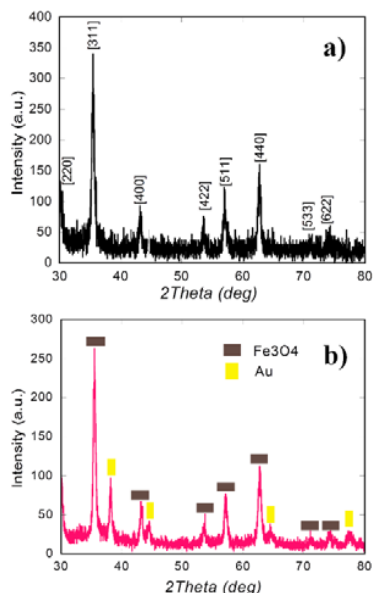


Fig. 2 XRD patterns of  $\text{Fe}_3\text{O}_4$  (a) and  $\text{Au}@/\text{Fe}_3\text{O}_4$  (b) nanoparticles synthesized by pulsed plasma in liquid

Fig. 3 represents a surface view of  $\text{Fe}_3\text{O}_4$  nanoparticles measured by HR-TEM. As shown in image, nanoparticles have an average diameter of  $\approx 18$  nm and majority of particles are nearly spherical in shape.

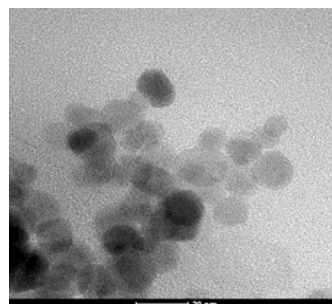


Fig. 3 Surface view of  $\text{Fe}_3\text{O}_4$  nanoparticles synthesized by pulsed plasma in liquid, taken by HR-TEM

Fig. 4 shows HR-TEM micrograph (a) of  $\text{Au}@/\text{Fe}_3\text{O}_4$  nanoparticles with the line profile (b and c) of the image contrast. The Au nanoparticles appear black and  $\text{Fe}_3\text{O}_4$  are light colored in the image, because Au has a higher electron density and allows fewer electrons to transmit. The interplanar d-spacings of the  $\text{Au}@/\text{Fe}_3\text{O}_4$  nanoparticles were calculated to be 3.48 nm ( $d=2.9670\text{\AA}$ ) for  $\text{Fe}_3\text{O}_4$  part and 2.34 nm ( $d=2.3548\text{\AA}$ ) for Au part, in a good agreement with the (220) and (111) planes of face centered cubic structured  $\text{Fe}_3\text{O}_4$  and Au (Fm-3m: 225), respectively.

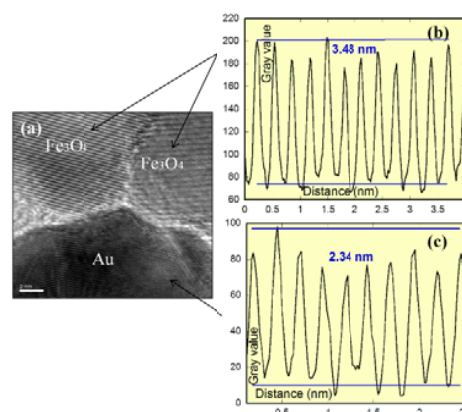


Fig. 4 HR-TEM results (a) high magnification view of  $\text{Au}@/\text{Fe}_3\text{O}_4$  nanoparticles (b) line profile image contrast for  $\text{Fe}_3\text{O}_4$  and (c) for Au

HR-TEM was equipped with an Energy dispersive spectrum (EDS) detector for elemental analysis. Fig. 5 displays the elemental compositions of samples: a)  $\text{Fe}_3\text{O}_4$  and b)  $\text{Au}@/\text{Fe}_3\text{O}_4$  nanoparticles. The composition of the magnetic phase ( $\text{Fe}_3\text{O}_4$ ) is 43% of Fe and 57% of oxygen; copper and carbon peaks are due to the sample holder, made of copper mesh coated with carbon. Thus, this confirms that, absent the presence C and Cu peaks due to the TEM micro-grid, the nanoparticles were composed solely of Fe and O. The presence of  $\text{Au}@/\text{Fe}_3\text{O}_4$  particles in the sample b) was confirmed indicating that besides C and Cu peaks only Fe, O and Au (b) were detected.

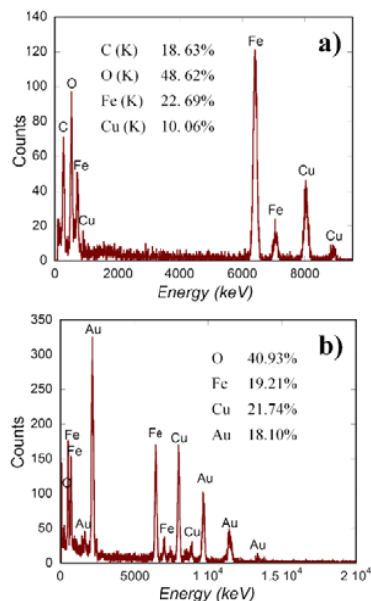


Fig. 5 EDS pattern of magnetite (a) and Au@Fe<sub>3</sub>O<sub>4</sub> (b) nanoparticles

Magnetic properties of NPs are strongly influenced by many parameters, including crystallinity, size, shape and crystal defects. Fig. 6 represents ferromagnetic behavior of magnetite (green line) and Au@Fe<sub>3</sub>O<sub>4</sub> (red line) NPs with low saturation magnetization measured by VSM at room temperature. Surprisingly, magnetic properties of magnetite remained in Au@Fe<sub>3</sub>O<sub>4</sub> nanoparticles, even though Au is non magnetic material. As a matter of function, in many cases the protecting shells not only act to stabilize the magnetic iron oxide NPs, but also may be used for further functionalization, in other words, gold can both provide stability for the magnetic NPs in solution as well as provide a good inert surface to assist in the binding of various biomolecules. Saturation magnetization ( $M_s$ ) at room temperature decreases sharply with decreasing crystalline size  $D$ , which was first pointed out by Berkowitz and co-workers in the late sixties [9].

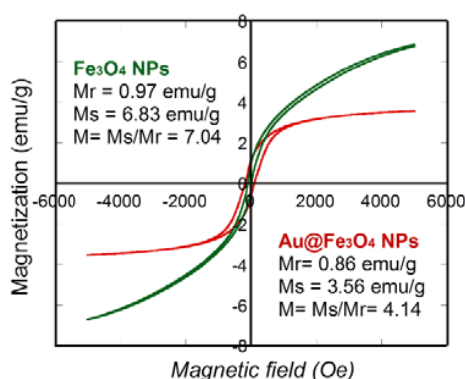


Fig. 6 Hysteresis loop of magnetization ( $M$ ,  $\text{emu g}^{-1}$ ) versus magnetic field ( $H$ , Oe) for magnetite ( $\text{Fe}_3\text{O}_4$ ) and Au@Fe<sub>3</sub>O<sub>4</sub> nanoparticles

Magnetic nanoparticles have been of significant use for

many different technological areas, especially in biomedical applications [10]. However, for use in biological system they should have among other properties biocompatibility with cells and tissues. Cytotoxicity of Fe<sub>3</sub>O<sub>4</sub> and Au@Fe<sub>3</sub>O<sub>4</sub> nanoparticles synthesized by PPL was evaluated by using a mammalian endothelial cell line, HeLa cells. HeLa cells are commonly used for testing the toxicity and trafficking of nanoparticles [11]. The Fig. 7 shows representative results obtained from the measurements. HeLa cells were exposed to magnetite (Fe<sub>3</sub>O<sub>4</sub>) and Au@Fe<sub>3</sub>O<sub>4</sub> NPs for 24 h. Suspensions of nanoparticles with concentration of 25, 50, 100 and 200  $\mu\text{g ml}^{-1}$  (Table I) were prepared by serial dilution. Cytotoxic effects were determined using a sodium 3'-] 1-(phenylaminocarbonyl)-3, 4-tetrazolium] bis (4-methoxy-6-nitro) benzenesulfonic acid hydrate (XTT; molecular formula: C<sub>22</sub>H<sub>16</sub>NaO<sub>13</sub>S<sub>2</sub>) assay kit. The organics used in the XTT assay are more stable and give more accurate results. The cell viability (%) was calculated according to the following equation:

$$\text{Cell viability (\%)} = \text{OD (sample)} / \text{OD (control)} \times 100$$

where OD (sample) represents the optical density of the wells treated with Fe<sub>3</sub>O<sub>4</sub> and Au@Fe<sub>3</sub>O<sub>4</sub> samples of various concentrations, OD (control) represents that of the wells treated with Dulbecco's modified eagle medium (D-MEM). The cytotoxicity assay results indicate that magnetite and Au@Fe<sub>3</sub>O<sub>4</sub> nanoparticles have a negligible effect on cells; indeed, cell viability was slightly higher with Au@Fe<sub>3</sub>O<sub>4</sub> nanoparticles than with Fe<sub>3</sub>O<sub>4</sub> nanoparticles. This demonstrates their potential for nanomedicine and biotechnological applications.

TABLE I  
CYTOTOXICITY OF MAGNETITE AND AU@Fe<sub>3</sub>O<sub>4</sub> NPS

Concentration ( $\mu\text{g mL}^{-1}$ )	Cell viability (%)	
	Fe <sub>3</sub> O <sub>4</sub>	Au@Fe <sub>3</sub> O <sub>4</sub>
25	98	99
50	95	99
100	95	98
200	89	91

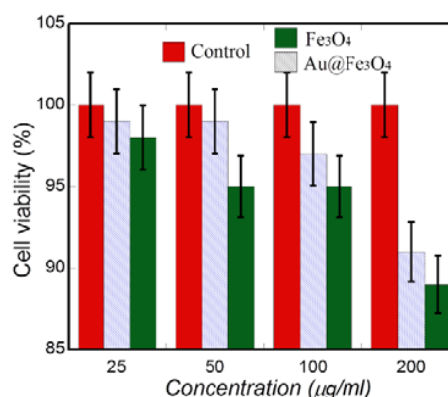


Fig. 7 Cytotoxicity of Fe<sub>3</sub>O<sub>4</sub> (green) and Au@Fe<sub>3</sub>O<sub>4</sub> (gray) nanoparticles prepared by pulsed plasma in liquid

## IV. CONCLUSION

Based on this study the following conclusions can be drawn:

1. Magnetite ( $\text{Fe}_3\text{O}_4$ ) and  $\text{Au}@\text{Fe}_3\text{O}_4$  NPs were synthesized by a simple, inexpensive method- pulsed plasma in liquid.
2. X-ray diffraction analysis indicated cubic structure of  $\text{Fe}_3\text{O}_4$  with  $a=8.296\text{\AA}$  (Fd-3m) for the sample (a); and a combination of cubic  $\text{Fe}_3\text{O}_4$  with Au phase (Fm-3m;  $a=4.079\text{\AA}$ ) for the sample (b).
3. Nanoparticles of  $\text{Fe}_3\text{O}_4$  have a spherical shape with average size of 19nm, and  $\text{Au}@\text{Fe}_3\text{O}_4$  nanoparticles combine spherical shaped Au and  $\text{Fe}_3\text{O}_4$  particles which proven by interplanar d-spacings calculated from HR-TEM image results.
4. VS-Magnetometer revealed weak ferromagnetic behavior of nanoparticles at room temperature.
5. Cytotoxicity assay results indicate that nanoparticles of  $\text{Fe}_3\text{O}_4$  and  $\text{Au}@\text{Fe}_3\text{O}_4$  synthesized by pulsed plasma in liquid have no effect on the cells, demonstrating their potentiality for biotechnological (-medical) applications.

group of Prof. T. Mashimo at the New Frontier Science department. Her research focuses on the synthesis of nanostructured materials using pulsed plasma in liquid method and novel properties of prepared materials.

## ACKNOWLEDGMENT

This work was partially supported by the Graduate School of Science and Technology of Kumamoto University.

We gratefully acknowledge E. T. Murzabekova for her valuable advices. The English was edited by William Baerg.

## REFERENCES

- [1] T. Matsunaga, Yoshiko Okamura and Tsuyoshi Tanaka "Biotechnological application of nano-scale engineered bacterial magnetic particles" *J. Mater. Chem.* 14 (2004) 2099-2105.
- [2] S. Bucak, D. A. Jones, P. E. Laibinis and T. A. Halton "Protein separation using colloidal magnetic nanoparticles" *Biotech Prog.* 2 (2003) 477-84.
- [3] M. Koneracka, P. Kopcansky, M. Timko and C. N. Ramshand "Direct binding procedure of proteins and enzymes to fine magnetic particles" *J Magn Magn Mater* 252 (2002) 409-11.
- [4] Z. G. Forbes, B. B. Yellen, K. A. Barbee and G. Friedman "AN approach to targeted drug delivery based on uniform magnetic fields" *IEEE trans Mag* 39 (2003) 3372-2 .
- [5] R. B. Gupta, U. B. Kompella "Nanoparticle technology for drug delivery" Taylor and Francis Group, New York, 2006, 416p.
- [6] E. Iglesias-Silva, J. L. Vilas-Vilela et al "Synthesis of gold-coated iron oxide nanoparticles" *J Non-Crystalline Solids* 356 (2010) 1233-35.
- [7] A. J. Wagstaff et al "Cisplatin drug delivery using gold-coated iron oxide nanoparticles for enhanced tumor targeting with external magnetic fields" *Inorganica Chimica Acta* xxx (2012).
- [8] E. Omurzak et al "Synthesis method of nanomaterials by pulsed plasma in liquid" *J Nanosci. Nanotechnol* 7 (2007) 3157-9.
- [9] A. E. Berkowitz, W. J. Schuele and P. J. Flanders "Influence of crystallite size on the magnetic properties of acicular  $\gamma\text{-Fe}_2\text{O}_3$  particles" *J Appl Phys* 39 (1968) 1261-64.
- [10] Z. Li, M. Kawashita, T. Kudo and H. Kanetaka "Sol-gel synthesis, characterization and in vitro compatibility evaluation of iron nanoparticle encapsulating - silica microspheres for hyperthermia of cancer" *J Mater Sci. Mater Med* 23 (2012) 2461-9.
- [11] J. M. Landry et al "The genomic and transcriptomic landscape of a HeLa cell line" G3: Genes/Genomes/ Genetics. (Early online published) 2013 doi: 10.1534g3.113.005777.

**Zhazgul Kelgenbaeva** (PhD student) received her B.S. in chemistry from Kyrgyz State University named after I. Arabayev (Kyrgyz Republic) in 2010 and worked as a junior research assistant in the group of prof. Saadat Sulaimankulova (Institute of Chemistry and Chemical Technology), National Academy of Science of the Kyrgyz Republic. Currently she is a doctoral course student (D2) at Kumamoto University and she has a doctoral fellowship in the